

# Incorporation of sulfur with graphitic carbon nitride into copper nanoparticles toward supercapacitor application

## Article history:

Received: 21-07-2023

Revised: 23-09-2023

Accepted: 15-10-2023

Karamveer Sheoran<sup>a</sup>, Nishu Devi<sup>b</sup>, Samarjeet Singh Siwal<sup>c</sup>

**Abstract:** The incorporation of S-g-C<sub>3</sub>N<sub>4</sub> into CuNPs resulted in enhanced electrochemical performance. The introduction of sulfur facilitated the formation of a highly conductive network within the composite material, enabling effective charge transfer and improved specific capacitance. The g-C<sub>3</sub>N<sub>4</sub> matrix served as a support network, controlling the accumulation of CuNPs and delivering stability during electrochemical cycling. The optimized S-g-C<sub>3</sub>N<sub>4</sub>/CuNPs composite showed superior electrochemical performance, high specific capacitance, and enhanced cycling stability. In this study, a facile and scalable synthesis method was employed to fabricate S-g-C<sub>3</sub>N<sub>4</sub>/CuNPs composite materials on GCE. The resulting composites were characterized using different optical and microscopic techniques. The electrochemical performance of the nanocomposites was assessed via using different techniques such as cyclic voltammetry (CV), and galvanostatic charge-discharge (GCD) techniques. The S-g-C<sub>3</sub>N<sub>4</sub>/CuNPs nanocomposite exhibited excellent electrochemical properties with a specific capacitance of 1944.18 F/g at a current density of 0.5 A/g and excellent cycling stability. The resultant composite material exhibits excellent electrochemical performance, making it an advantageous nominee for energy storage applications needing high power density, extended cycling life, and steadfast performance.

**Keywords:** Graphitic carbon nitride; Copper nanoparticles; Energy storage application; Cyclic voltammetry.

<sup>a</sup> Department of Chemistry, M.M. Engineering College, Maharishi Markandeshwar (Deemed to be University), Mullana-Ambala, Haryana, 133207, India.

<sup>b</sup> Mechanics and Energy Laboratory, Department of Civil and Environmental Engineering, Northwestern University, 2145 Sheridan Road, Evanston, IL60208, USA.

<sup>c</sup> Department of Chemistry, M.M. Engineering College, Maharishi Markandeshwar (Deemed to be University), Mullana-Ambala, Haryana, 133207, India. Department of Chemical Engineering Technology, University of Johannesburg, P.O. Box 17011, Doornfontein, 2088, South Africa. Corresponding author: samarjeet6j1@gmail.com

## 1. INTRODUCTION

With the continuous shortage of fossil fuels, rapidly changing environment changes, irregular allocation of energy and universal ecological contamination crises, there has always been a need to generate more hygienic, renewable and steadfast energy origins to manage the ever-growing energy demands of the human being (Mishra, Devi, Siwal, & Thakur, 2023; Mishra *et al.*, 2022). To address these necessary energy needs, more efficient, cost-effective, alternative energy storage solutions are needed to quickly harness energy from irregular renewable sources such as solar, wind, and hydropower and store it (González, Goikolea, Barrena, & Mysyk, 2016; Karamveer, Thakur, & Siwal, 2022; Kim, Kim, Choi, Park, & Shin, 2020; Samarjeet Singh Siwal *et al.*, 2022; G. Wang, Zhang, & Zhang, 2012). An electrochemical energy storage/conversion approach is one such innovation. Electrochemical capacitors, also known as supercapacitors (SCs) or ultracapacitors, have gained prominence due to their exceptional properties;

they have higher power densities (PDs) than traditional batteries and can store ten to a hundred times more energy over a short period compared to capacitors. They tend to have thousands of ongoing GCD cycles, distinguishing them from other storing gadgets like batteries and SCs (Ashritha & Hareesh, 2020; X. Li & Wei, 2013; Najib & Erdem, 2019; S. Samarjeet Siwal, Zhang, Devi, & Thakur, 2020).

Graphitic carbon nitride ( $g\text{-C}_3\text{N}_4$ ) with a two-dimensional (2D) graphite-alike network has drawn much awareness as an the effective dynamic material for SC due to its nitrogen-rich composition, excellent thermal and chemical stability, eco-friendliness, and ease of preparation (Mishra, Devi, Siwal, Gupta, & Thakur, 2023; Qiu *et al.*, 2022; Y. Xu, Zhou, Guo, Zhang, & Lu, 2019). However, its intrinsic lower electronic performance and surface area limit the electrochemical activity of  $g\text{-C}_3\text{N}_4$  (Ghaemmaghami & Mohammadi, 2019; Luo, Yan, Zheng, Xue, & Pang, 2019; Samarjeet Singh Siwal, Zhang, Sun, & Thakur, 2019). Various methods are used to improve the electronic performance and surface area of  $g\text{-C}_3\text{N}_4$  for enhancing its energy storage capability, including network assembly (Oh, Kim, Choi, & Kim, 2018; Shen *et al.*, 2018), heteroatom doping (Kong *et al.*, 2017; Y. Li *et al.*, 2019) hybrid with metal combinations (Z. Li, Wu, Wang, Gu, & Zhou, 2017; Ma, Yang, Kubendhiran, & Lin, 2022).

To enhance the energy storage capacity of  $g\text{-C}_3\text{N}_4$ , it is suitable to employ various methods simultaneously, such as heteroatom incorporation and metal combination integration. Additionally, sulfur plays a crucial role in improving SC's specific capacitance and cycle stability with different sulfur vacancies and contaminants (J. Xu *et al.*, 2021). Thus, doping sulfur into  $g\text{-C}_3\text{N}_4$  and containing CuNPs within  $g\text{-C}_3\text{N}_4$  are very appealing to manufacturing effective active material of SC. The higher energy density and specific capacitance of pseudocapacitors have attracted attention in the energy storage field in recent years (Tyagi, Myung, Tripathi, Kim, & Gupta, 2020; Tyagi, Singh, Sharma, & Gupta, 2019). Carbon cloth has also gained considerable interest for designing flexible supercapacitor electrodes due to its strong mechanical stability, particular 3D structure, noticeable electrical conductivity, flexibility, and cost-effectiveness (Tyagi, Chandra Joshi, Agarwal, Balasubramaniam, & Gupta, 2019; Tyagi, Joshi, Shah, Thakur, & Gupta, 2019).

In this work, a facile synthesis method of  $g\text{-C}_3\text{N}_4$  is supported with CuNPs and anchored with Sulphur. This electrode assembly demonstrates

improved electrochemical performance of the S- $g\text{-C}_3\text{N}_4$ /CuNPs nanocomposite, attributed to the synergistic effects of the Sulphur source and CuNPs, and the  $g\text{-C}_3\text{N}_4$ , which provides high surface area and good conductivity. This paper is divided into two fractions: the first provides information related to the material's characterization, and the second elucidates the electrochemical activity of the synthesized material for SCs application.

## 2. EXPERIMENTS

### 2.1. Chemical and substances

Copper sulfate pentahydrate ( $\text{CuSO}_4 \cdot 5\text{H}_2\text{O}$  (s),  $\geq 98\%$ ), Urea ( $\text{CH}_4\text{N}_2\text{O}$ ,  $\geq 99\%$ ), thiourea ( $\text{CH}_4\text{N}_2\text{S}$ ,  $\geq 99\%$ ), Nafion (5%) and other substances were obtained from Merck, USA. Monosodium ( $\text{NaH}_2\text{PO}_4$  (s),  $\geq 99\%$ ) and disodium phosphate ( $\text{Na}_2\text{HPO}_4$  (s),  $\geq 98.5\%$ ), potassium ferricyanide ( $\text{K}_3\text{Fe}(\text{CN})_6$  (s),  $\geq 99\%$ ), potassium ferrocyanide ( $\text{K}_4\text{Fe}(\text{CN})_6$  (s),  $\geq 99\%$ ), potassium hydroxide (KOH (s),  $> 99\%$ ), and ethyl acetate ( $\text{C}_4\text{H}_8\text{O}_2$  (l),  $> 98\%$ ) were also acquired from Merck. All chemicals were used without further purification.

### 2.2. Synthesis of $g\text{-C}_3\text{N}_4$ and $g\text{-C}_3\text{N}_4$ /CuNPs nanocomposites

Fresh  $g\text{-C}_3\text{N}_4$  was prepared using heating urea (CDH, 98.0%) into the air at 500 °C for 5 h with a heating velocity of 5 °C/min for polymerization (S. Siwal *et al.*, 2018; S. Siwal, Devi, Perla, Ghosh, & Mallick, 2019). In the synthesis, 20 g urea was placed within a crucible and transferred to a muffle furnace. The urea was heated in air at 550 °C for 5 h with a heating velocity of 5 °C/min. Similarly, the S- $g\text{-C}_3\text{N}_4$ /CuNPs with S-doping were obtained.

The  $g\text{-C}_3\text{N}_4$ /CuNPs nanocomposite was synthesized using a one-step reduction approach. A 0.5 M precursor of  $\text{CuSO}_4 \cdot 5\text{H}_2\text{O}$  was counted dropwise (5 wt% incorporation of Cu) to a flask in a specific synthesis. Subsequently, 5 mL of  $1 \times 10^{-3}$  M  $\text{NaBH}_4$  solution was measured in a dropwise flask to reduce the copper salt. Finally, the material was purified, cleaned with water, and dried. The resulting material,  $g\text{-C}_3\text{N}_4$ /CuNPs, was illustrated employing various approaches and used as a catalyst for the SC application. Similarly, S- $g\text{-C}_3\text{N}_4$ /CuNPs (5.0 mol% of Cu loading) were also prepared to employ the precursors of  $\text{CuSO}_4 \cdot 5\text{H}_2\text{O}$  and thiourea solution. Thiourea ( $0.1 \text{ mol dm}^{-3}$ ) was added to this reaction

combination and permitted to agitate for 1 h. The whole reaction was achieved under atmospheric circumstances. The greenish precipitate material was permitted to gather for 30 min, after which the settled material was taken from the bottom of the container and pipetted upon lacey, carbon-painted, Cu mesh grids for transmission electron microscopy (TEM) analysis. The residual part of the mixture was dried underneath a vacuum at 60 °C for Electrochemical studies and used as a substance for the SC application.

### 2.3. Incorporating electrodes and symmetric supercapacitor

The SC electrode was designed using incorporating an electrocatalyst on a glassy carbon electrode (GCE, 5 mm). The GCE was cleaned according to our earlier analysis (S. S. Siwal *et al.*, 2019). The  $g\text{-C}_3\text{N}_4$ ,  $g\text{-C}_3\text{N}_4/\text{CuNPs}$ , and  $S\text{-}g\text{-C}_3\text{N}_4/\text{CuNPs}$  nanocomposites are active materials. The conductive mixture was prepared by combining using the active material and Nafion with the ratio of 8: 1 in ethyl acetate underneath agitating at ambient condition for 4 h. After applying the electrocatalyst to the GCE, the electrode was warmed at 60 °C 4 h. The electrochemical system was established using three-electrode system for SC characterization in 1 M KOH media.

### 2.4. Material characterizations

TEM analyses were conducted at an increasing voltage of 197 kV utilizing a Philips CM200 TEM apparatus fitted with a  $\text{LaB}_6$  source. The TEM specimens were designed by placing a small amount of prepared material on a TEM grid (200 mesh size Cu-grid) covered with a lacy carbon sheet. FTIR spectra were collected using a Shimadzu IRAffinity-1 with a spectral resolution of  $0.5\text{ cm}^{-1}$ . The UV-Vis spectra were measured using a Shimadzu UV-1800 spectrophotometer with a quartz cuvette. The electrochemical activity of SC electrodes was analyzed in a three-electrode electrochemical technique, where the GCE was employed as the working electrode, the Pt wire served as a counter electrode, and Hg/HgO electrode was applied as the reference electrode in 1 M KOH as electrolyte. The CV, GCD, and electrochemical impedance spectroscopy (EIS) were measured using a potentiostat/galvanostat apparatus fitted with a Shanghai Chenhua 760 E potentiostat into a single-cell three-electrode system

within a 1 M KOH solution. The EIS measurements were conducted at open-circuit voltage with frequency ranges from 0.01 Hz to 100 kHz.

## 3. RESULTS AND DISCUSSION

### 3.1. Material characterizations

The prepared material was characterized using various structural, morphological, and optical analyses. In a typical synthetic method described into this study, 20 g of urea was directly calcinated in a 50 ml crucible in a muffle furnace. The vessel was semi-sealed, heated and stocked at the terminal calcination temperature is around ( $T = 500\text{ °C}$ ) for 3 h. The  $g\text{-C}_3\text{N}_4/\text{CuNPs}$  (5.0 mol% of Cu) were prepared using  $\text{CuSO}_4 \cdot 5\text{H}_2\text{O}$  precursor through a one-step  $\text{NaBH}_4$  reduction process at ambient conditions. A greenish colloidal material was created during the accumulation of copper salt. The entire reaction was conducted under environmental essentials for 120 min. Throughout the reaction, a greenish material precipitated at the bottom of the container. The graphic depiction of the synthesis process of  $S\text{-}g\text{-C}_3\text{N}_4/\text{CuNPs}$  nanocomposite material is shown in Fig. 1(a). Fig. 1(b) illustrates the potential electrochemical energy storage application of synthesized material.

To check the understanding of the synthesized material, we characterized the synthesized material using TEM. Fig. 2(a, b) demonstrates the TEM images of  $S\text{-}g\text{-C}_3\text{N}_4/\text{CuNPs}$  materials at different magnifications.

In Fig. 3, the FTIR analysis of powder and thin sheet specimens revealed a characteristic peak at  $807\text{ cm}^{-1}$ , which corresponds to the vibration of heptazine groups (Huang *et al.*, 2021), The CN hexagonal rings were observed through high-intensity multiple peak in the  $1200\text{--}1400\text{ cm}^{-1}$  range, associated with the C–N and C = N bonds (X. Wang *et al.*, 2009). The peak at  $1115\text{ cm}^{-1}$  was allied with C–O stretching, evidenced by oxygen-based functional groups. Additionally, the peak at  $1635\text{ cm}^{-1}$  was indicative of N–H bending, and the broad peak range of  $3000\text{--}3300\text{ cm}^{-1}$  was associated with N–H stretching (Ahmad Kamal, Ritikos, & Abdul Rahman, 2015; Liu, Wang, & Antonietti, 2016). Based on the FTIR data, our direct development samples possessed satisfactory O-based and NH groups, which significantly contributed to their superhydrophilic behavior. Notably, the simultaneousness of O-based groups and NH groups was occasional because oxygen could respond selectively with hydrogen instead of

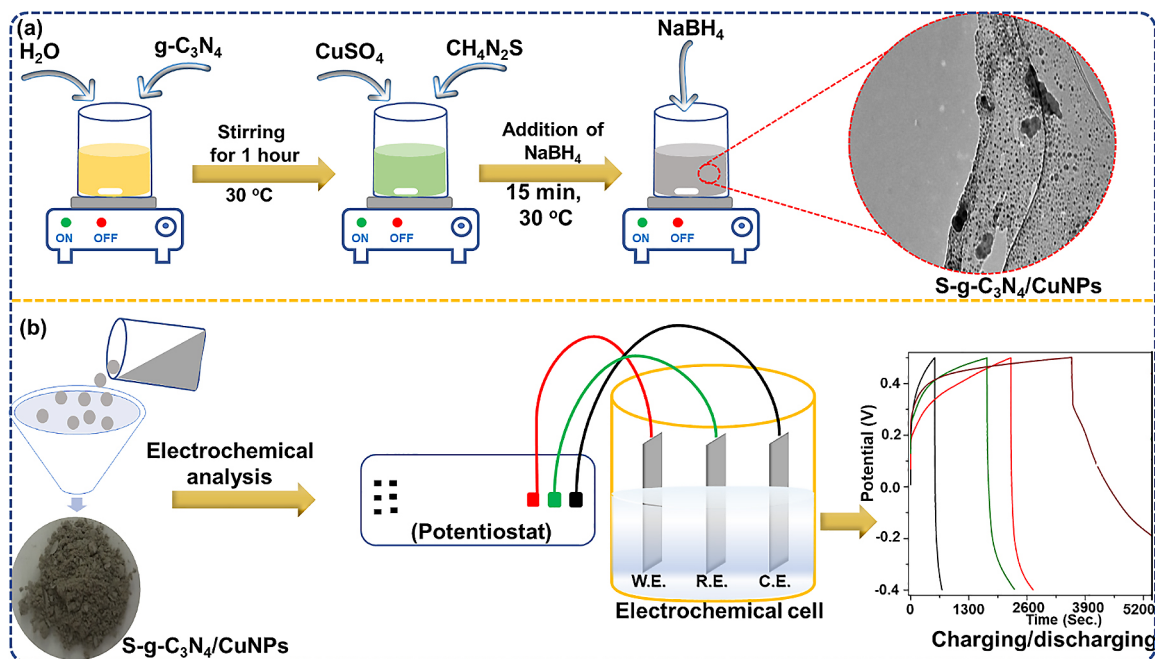


**Fig. 1.** (a) Displays the graphic illustration of the synthesis process of S-g-C<sub>3</sub>N<sub>4</sub>/CuNPs composite material. (b) Shows the graphical representation electrochemical energy storage application of synthesized material.

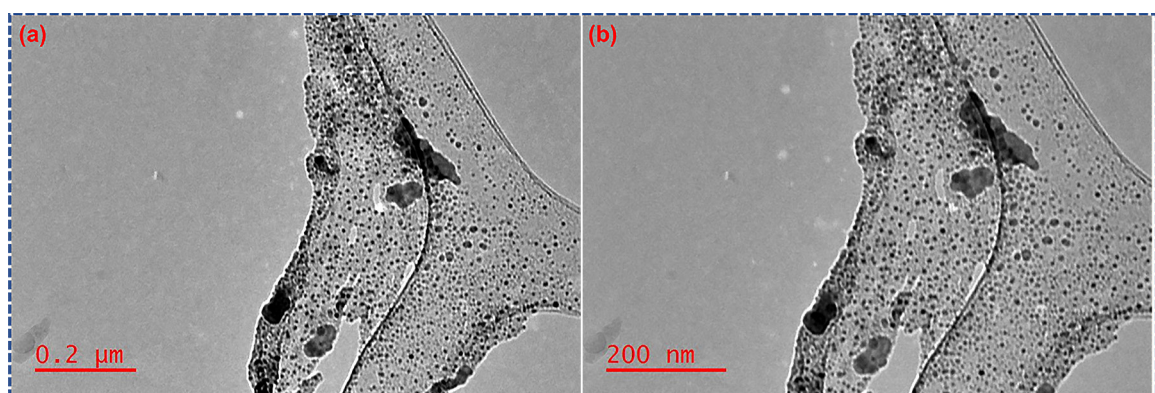


**Fig. 2.** (a & b) Shows the TEM pictures of S-g-C<sub>3</sub>N<sub>4</sub>/CuNPs composite material.

attaching to the surface. This determined the ratio of O-based groups implanted to the surface. However, this constraint was absent in the proposed synthesis method because these functional groups were spontaneously integrated during the polycondensation of samples instead of existing embedded after preparation. The chemical bonds within thin films closely resembled those in the powder specimens, in powder specimens except for the higher ratio of C≡N bonds peaking at 2170 cm<sup>-1</sup> (Thi *et al.*, 2023).

The optical effects of the prepared NPs were examined (Fig. 4) by dispersing the materials in DI water. The essential sharp absorption band edges are

sequentially marked for g-C<sub>3</sub>N<sub>4</sub> at 370 and 460 nm. It observed that upon the incorporation of varying amounts of g-C<sub>3</sub>N<sub>4</sub> to the CuNPs, the absorption peaks were red-shifted from the UV to the visible area. This shift signifies the formation of heterojunction nanocomposites and demonstrates a correlation between the g-C<sub>3</sub>N<sub>4</sub> content and the absorption intensity (Radoń & Łukowiec, 2018; Xue, Ma, Zhou, Zhang, & He, 2015). The UV-Vis absorption of the specimens also improved with rising g-C<sub>3</sub>N<sub>4</sub> content. This indicates a risen electric exterior charge upon the oxide into the nanocomposite owing to the preface introduction of g-C<sub>3</sub>N<sub>4</sub> (Ghorui *et al.*, 2021).



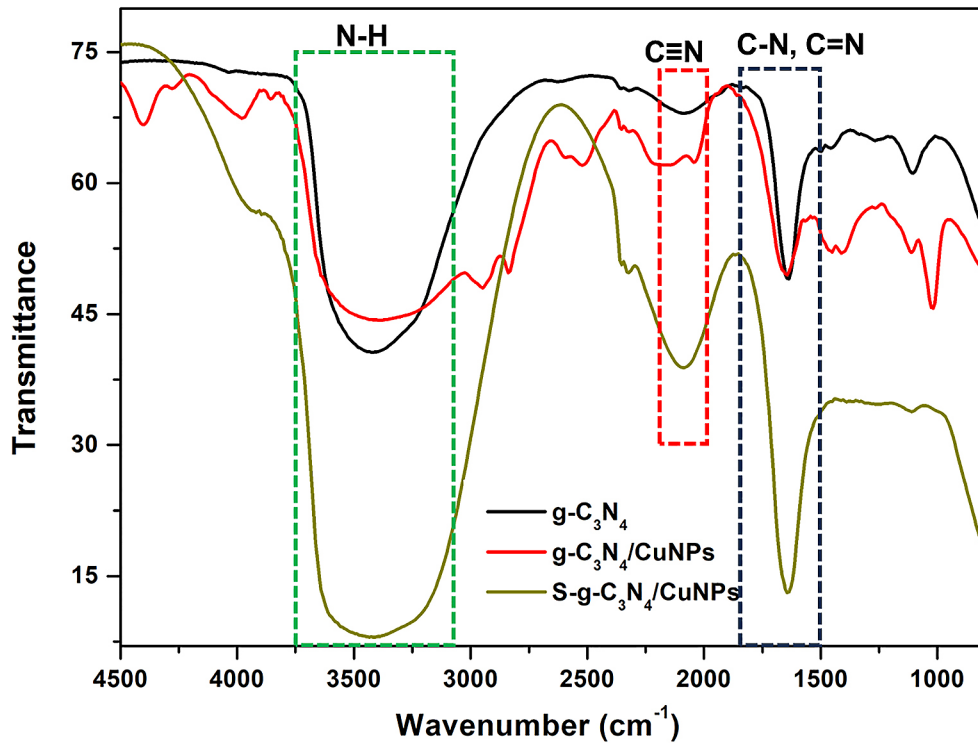


Fig. 3. FTIR spectra of g-C<sub>3</sub>N<sub>4</sub>, g-C<sub>3</sub>N<sub>4</sub>/CuNPs and S-g-C<sub>3</sub>N<sub>4</sub>/CuNPs.

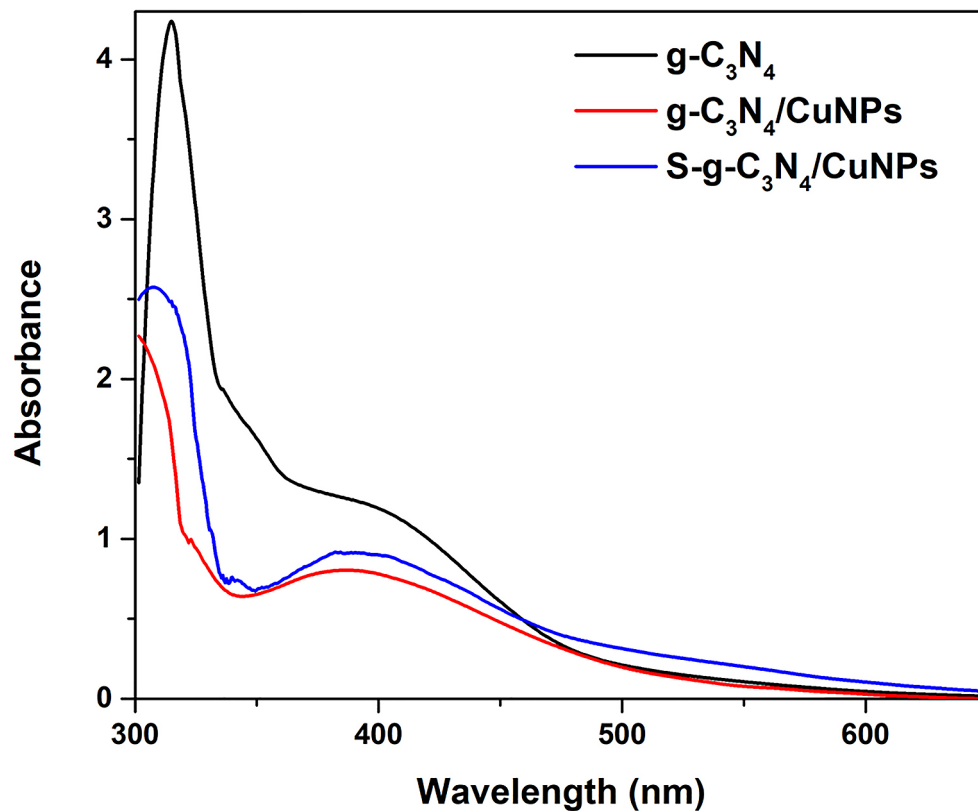


Fig. 4. UV-Vis spectra of g-C<sub>3</sub>N<sub>4</sub>, g-C<sub>3</sub>N<sub>4</sub>/CuNPs and S-g-C<sub>3</sub>N<sub>4</sub>/CuNPs.

GCD curves of all incorporated electrodes in the voltage range of -0.4 to 0.45V with distinct current densities (CDs) are shown in Fig. 5(a). The graph showed the high charge-storage capability of S-g-C<sub>3</sub>N<sub>4</sub>/CuNPs material. The specific capacitance of the proposed material was calculated by the subsequent equation (Radhamani, Shareef, & Rao, 2016):

$$C_s = (i * \Delta t) / (m * \Delta V)$$

$$ED = (i * \Delta V * \Delta t * 1000) / (m * 3600)$$

$$PD = (i * \Delta V * 1000) / m$$

$$\eta = (t_d / t_c) * 100$$

Where  $C_s$  denotes the specific capacitance of the nanocomposite in F/g, energy density (ED) in Wh/kg, power density (PD) in W/kg, coulombic efficiency in %,  $\Delta t$  denotes the liberation period in seconds,  $\Delta V$  is the voltage dissimilarity in V,  $i$  is the

current used to the electrode in A and  $m$  as the mass of electrode on GCE surface in gram thus  $i/m$  is the CD of the system in A/g. The highest specific capacitance for the proposed material was 1944.18 F/g at 0.5 A/g.

CV is an advanced approach for evaluating the behavior of active redox substances. In the initial phase, it allows for identifying whether the material behaves as an electric double-layer capacitor (EDLC) or exhibits pseudocapacitive characteristics. Fig. 5(b) illustrates the CV of S-g-C<sub>3</sub>N<sub>4</sub>/CuNPs nanocomposite at distinct sweep rates from 20 mV/s to 200mV/s. The progressively raised CD value with constantly repeated scan rates from 20 mV/s to 200 mV/s resulted in a shift in the peak voltage value, showing the material's enhanced performance by shifting the peak upward at the same voltage.

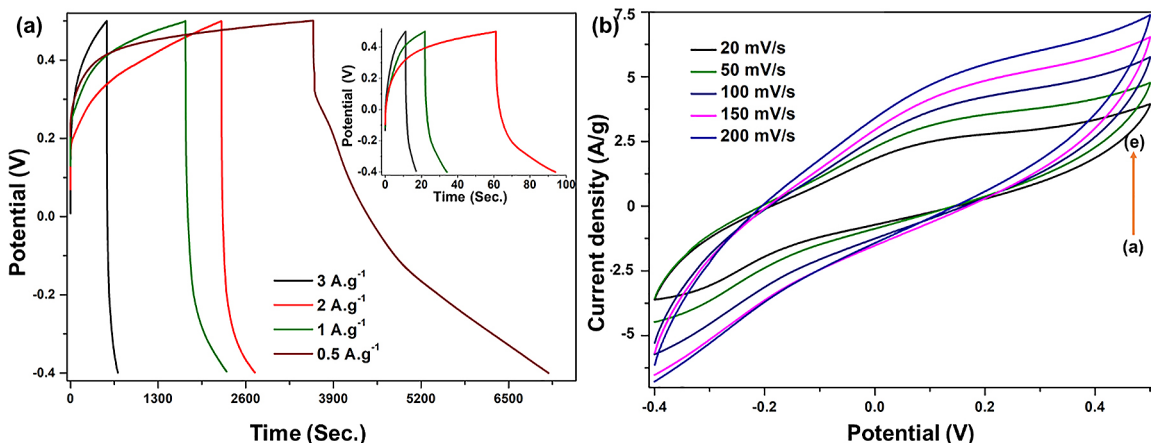


**Fig. 5.** (a) GCD analysis of S-g-C<sub>3</sub>N<sub>4</sub>/CuNPs nanocomposite at distinct CDs (inset: g-C<sub>3</sub>N<sub>4</sub>/CuNPs). (b) CV analysis of S-g-C<sub>3</sub>N<sub>4</sub>/CuNPs nanocomposite at distinct sweep rates.

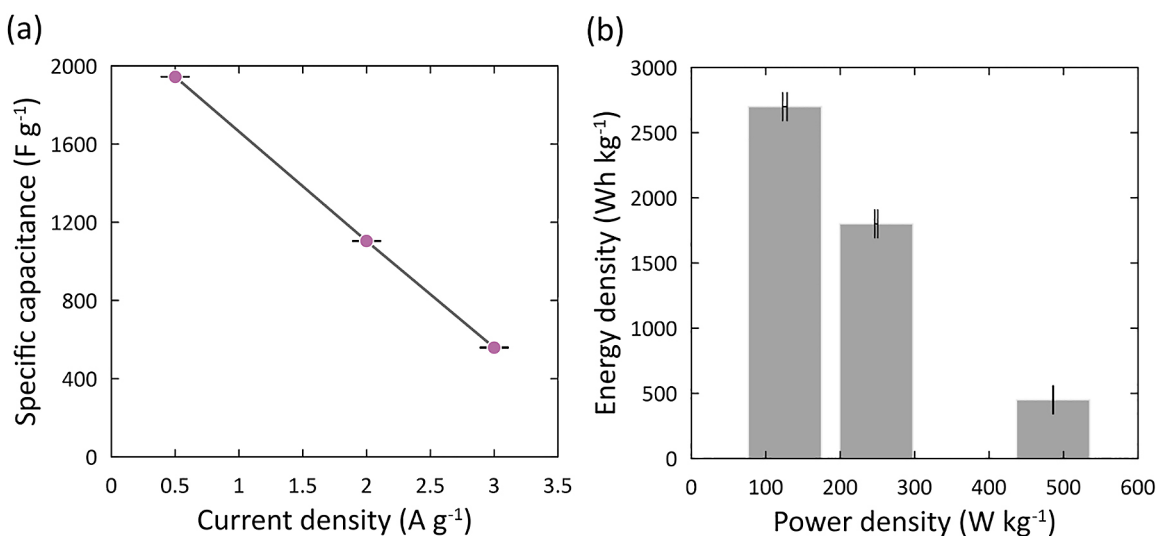
The decrease in specific capacitance during the cycling method can be attributed to the material's mechanical fatigue effects generated through the constant loading and unloading of the ions from the media. A reverse pattern has been marked for the S-g-C<sub>3</sub>N<sub>4</sub>/CuNPs incorporated electrode, where an increase in specific capacitance value has been noted for various charge-discharge cycles (Table 1).

Fig. 6(a) shows the specific capacitance of S-g-C<sub>3</sub>N<sub>4</sub>/CuNPs nanocomposite at different CD values. Error bar diagram, which maps the ED and PD, of S-g-C<sub>3</sub>N<sub>4</sub>/CuNPs nanocomposite symmetric cells by varying current densities (0.5, 2, and 3 A g<sup>-1</sup>) are demonstrated in Fig. 6(b).

Long-term stability is a critical factor influencing the practical utility of SCs, and the cyclic strength of prepared nanocomposite material is a crucial parameter for determining its suitability for practical applications. As demonstrated in Fig. 7, the cycling stability plots from more than 100 repetitive GCD cycles showed a high performance with redundant methods. The S-g-C<sub>3</sub>N<sub>4</sub>/CuNPs nanocomposite is a suitable electrode substance for SC incorporation to improve cyclic stability. It has been monitored that adequate cyclic stability offers around 95% capacitance retention for 200 cycles. The first 23 longer CD cycles at a CD 3 A/g are given in Fig. 7(a).

Materials	Current density [A/g]	Specific capacitance [F/g]	Energy density [Wh/kg]	Power density [W/kg]	Ref.
Nickel cobalt sulfide/porous g-C <sub>3</sub> N <sub>4</sub> /activated carbon	1	506 C/g	16.7	200	(Z. Li <i>et al.</i> , 2017)
g-C <sub>3</sub> N <sub>4</sub> /graphene	0.4	264	30	4 kW/kg	(Chen, Zhao, Huang, Chen, & Qu, 2015)
3D oxidized g-C <sub>3</sub> N <sub>4</sub> /graphene	1	265.6	14.93	571.36	(Lin <i>et al.</i> , 2017)
Carbon cloth@ g-C <sub>3</sub> N <sub>4</sub> -900	1	499	10.1	10000	(J. Zhu <i>et al.</i> , 2020)
Bismuth ferrite/ g-C <sub>3</sub> N <sub>4</sub> -doped graphene quantum dots	1	1472	53.1	705.4	(Shalini Reghunath <i>et al.</i> , 2022)
Co <sub>3</sub> O <sub>4</sub> /g-C <sub>3</sub> N <sub>4</sub>	1.25	780	—	—	(H.-L. Zhu & Zheng, 2018)
Porous g-C <sub>3</sub> N <sub>4</sub> nanosheets	0.1	520	—	—	(H. Wang <i>et al.</i> , 2023)
CoFe <sub>2</sub> O <sub>4</sub> /Cu/g-C <sub>3</sub> N <sub>4</sub>	1	1380	144.4	7.992 kW/kg	(Yesmin, Devi, Dasgupta, & Dhar, 2022)
S-g-C <sub>3</sub> N <sub>4</sub> /CuNPs	3	559.18	125.66	2700	This work
S-g-C <sub>3</sub> N <sub>4</sub> /CuNPs	2	1104.04	248.41	1800	This work
S-g-C <sub>3</sub> N <sub>4</sub> /CuNPs	0.5	1944.18	486.04	450	This work

**Table 1.** Shows the Comparison of supercapacitive performance of our material with the literature.



**Fig. 6.** (a) Specific capacitance of S-g-C<sub>3</sub>N<sub>4</sub>/CuNPs nanocomposite at different CD values. (b) Error bar of S-g-C<sub>3</sub>N<sub>4</sub>/CuNPs.

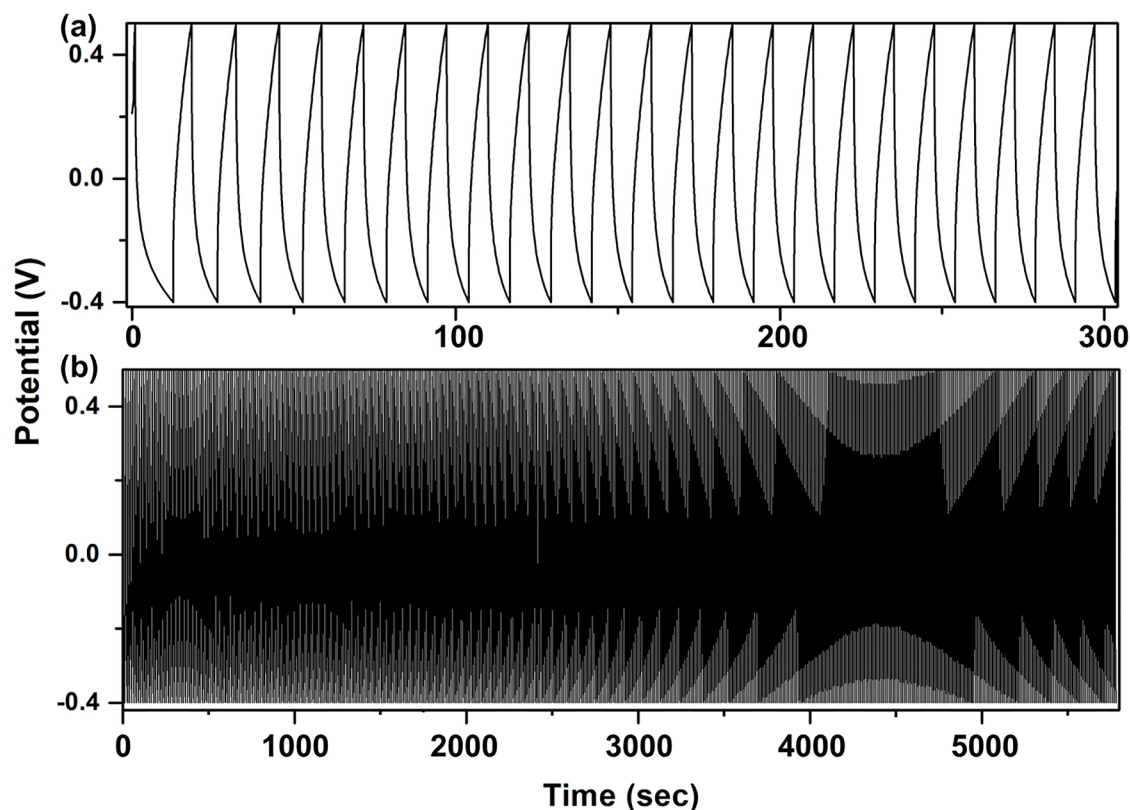


**Fig. 7.** (a) GCD curve for 23 consecutive cycles at CD 5 Ag<sup>-1</sup> and (b) Shows the 200 GCD cycle life stability of S-g-C<sub>3</sub>N<sub>4</sub>/CuNPs nanocomposite.

## CONCLUSION

In conclusion, the incorporation of sulfur with g-C<sub>3</sub>N<sub>4</sub> into CuNPs demonstrates significant potential for supercapacitor (SC) applications. The synergistic combination of these materials offers key advantages, including enhanced electrical conductivity, improved charge transfer kinetics, and an increased specific surface area, resulting in superior electrochemical performance.

Incorporating sulfur with g-C<sub>3</sub>N<sub>4</sub> into CuNPs confirms the excellent potential for developing high-performance SCs. This unique material combination strikes a balance between high energy density (ED) and power density (PD), making it suitable for a wide range of applications, such as portable electronics, hybrid vehicles, and renewable energy systems. Ongoing research and optimization of the synthesis methods and electrode structures will pave the way for the practical realization of this composite material in real-world SC appliances. Overall, S-g-C<sub>3</sub>N<sub>4</sub>/CuNPs provide a suitable pathway for developing next-generation SCs with

improved energy storage performance, cycling stability, and power output. These advancements have the potential to revolutionize energy storage technology and contribute to the progress of a better sustainable, and efficient future.

## Acknowledgement

The authors extend their gratitude for the support received from the Department of Chemistry and Research & Development Cell of Maharishi Markandeshwar (Deemed to be University), Mullana, Ambala, Haryana, India. ♦

## REFERENCES

- AHMAD KAMAL, S. A., RITIKOS, R., & ABDUL RAHMAN, S. (2015). Wetting behaviour of carbon nitride nanostructures grown by plasma enhanced chemical vapour deposition technique. *Applied Surface Science*, 328, 146-153. doi:https://doi.org/10.1016/j.apsusc.2014.12.001



- ASHRITHA, M. G., & HAREESH, K. (2020). A review on Graphitic Carbon Nitride based binary nanocomposites as supercapacitors. *Journal of Energy Storage*, 32, 101840. doi:https://doi.org/10.1016/j.est.2020.101840
- CHEN, Q., ZHAO, Y., HUANG, X., CHEN, N., & QU, L. (2015). Three-dimensional graphitic carbon nitride functionalized graphene-based high-performance supercapacitors. *Journal of Materials Chemistry A*, 3(13), 6761-6766. doi:10.1039/C5TA00734H
- GHAEMMAGHAMI, M., & MOHAMMADI, R. (2019). Carbon nitride as a new way to facilitate the next generation of carbon-based supercapacitors. *Sustainable Energy & Fuels*, 3(9), 2176-2204. doi:10.1039/C9SE00313D
- GHORUI, U. K., SATRA, J., MONDAL, P., MARDANYA, S., SARKAR, A., SRIVASTAVA, D. N., ... MONDAL, A. (2021). Graphitic carbon nitride embedded-Ag nanoparticle decorated-ZnWO<sub>4</sub> nanocomposite-based photoluminescence sensing of Hg<sup>2+</sup>. *Materials Advances*, 2(12), 4041-4057. doi:10.1039/D1MA00211B
- GONZÁLEZ, A., GOIKOLEA, E., BARRENA, J. A., & MYSYK, R. (2016). Review on supercapacitors: Technologies and materials. *Renewable and Sustainable Energy Reviews*, 58, 1189-1206. doi:https://doi.org/10.1016/j.rser.2015.12.249
- HUANG, C., WEN, Y., MA, J., DONG, D., SHEN, Y., LIU, S., ... ZHANG, Y. (2021). Unraveling fundamental active units in carbon nitride for photocatalytic oxidation reactions. *Nature Communications*, 12(1), 320. doi:10.1038/s41467-020-20521-5
- KARAMVEER, S., THAKUR, V. K., & SIWAL, S. S. (2022). Synthesis and overview of carbon-based materials for high performance energy storage application: A review. *Materials Today: Proceedings*, 56, 9-17. doi:https://doi.org/10.1016/j.matpr.2021.11.369
- KIM, E., KIM, S., CHOI, Y. M., PARK, J. H., & SHIN, H. (2020). Ultrathin Hematite on Mesoporous WO<sub>3</sub> from Atomic Layer Deposition for Minimal Charge Recombination. *ACS Sustainable Chemistry & Engineering*, 8(30), 11358-11367. doi:10.1021/acssuschemeng.0c03579
- KONG, L., CHEN, Q., SHEN, X., XIA, C., JI, Z., & ZHU, J. (2017). Ionic Liquid Templated Porous Boron-Doped Graphitic Carbon Nitride Nanosheet Electrode for High-Performance Supercapacitor. *Electrochimica Acta*, 245, 249-258. doi:https://doi.org/10.1016/j.electacta.2017.05.141
- LI, X., & WEI, B. (2013). Supercapacitors based on nanostructured carbon. *Nano Energy*, 2(2), 159-173. doi:https://doi.org/10.1016/j.nanoen.2012.09.008
- LI, Y., WANG, S., CHANG, W., ZHANG, L., WU, Z., SONG, S., & XING, Y. (2019). Preparation and enhanced photocatalytic performance of sulfur doped terminal-methylated g-C<sub>3</sub>N<sub>4</sub> nanosheets with extended visible-light response. *Journal of Materials Chemistry A*, 7(36), 20640-20648. doi:10.1039/C9TA07014A
- LI, Z., WU, L., WANG, L., GU, A., & ZHOU, Q. (2017). Nickel cobalt sulfide nanosheets uniformly anchored on porous graphitic carbon nitride for supercapacitors with high cycling performance. *Electrochimica Acta*, 231, 617-625. doi:https://doi.org/10.1016/j.electacta.2017.02.087
- LIN, R., LI, Z., ABOU EL AMAIEM, D. I., ZHANG, B., BRETT, D. J. L., HE, G., & PARKIN, I. P. (2017). A general method for boosting the supercapacitor performance of graphitic carbon nitride/graphene hybrids. *Journal of Materials Chemistry A*, 5(48), 25545-25554. doi:10.1039/C7TA09492B
- LIU, J., WANG, H., & ANTONIETTI, M. (2016). Graphitic carbon nitride "reloaded": emerging applications beyond (photo)catalysis. *Chemical Society Reviews*, 45(8), 2308-2326. doi:10.1039/C5CS00767D
- LUO, Y., YAN, Y., ZHENG, S., XUE, H., & PANG, H. (2019). Graphitic carbon nitride based materials for electrochemical energy storage. *Journal of Materials Chemistry A*, 7(3), 901-924. doi:10.1039/C8TA08464E
- MA, J.-S., YANG, H., KUBENDHIRAN, S., & LIN, L.-Y. (2022). Novel synthesis of sulfur-doped graphitic carbon nitride and NiCo<sub>2</sub>S<sub>4</sub> composites as efficient active materials for supercapacitors. *Journal of Alloys and Compounds*, 903, 163972. doi:https://doi.org/10.1016/j.jallcom.2022.163972
- MISHRA, K., DEVI, N., SIWAL, S. S., GUPTA, V. K., & THAKUR, V. K. (2023). Hybrid Semiconductor Photocatalyst Nanomaterials for Energy and Environmental Applications: Fundamentals, Designing, and Prospects. *Advanced Sustainable Systems*, n/a(n/a), 2300095. doi:https://doi.org/10.1002/adsu.202300095
- MISHRA, K., DEVI, N., SIWAL, S. S., & THAKUR, V. K. (2023). Insight perspective on the synthesis and morphological role of the noble and non-noble metal-based electrocatalyst in fuel cell application. *Applied Catalysis B: Environmental*, 334, 122820. doi:https://doi.org/10.1016/j.apcatb.2023.122820

- MISHRA, K., DEVI, N., SIWAL, S. S., ZHANG, Q., ALSANIE, W. F., SCARPA, F., & THAKUR, V. K. (2022). Ionic Liquid-Based Polymer Nanocomposites for Sensors, Energy, Biomedicine, and Environmental Applications: Roadmap to the Future. *Advanced Science*, 9(26), 2202187. doi:https://doi.org/10.1002/advs.202202187
- NAJIB, S., & ERDEM, E. (2019). Current progress achieved in novel materials for supercapacitor electrodes: mini review. *Nanoscale Advances*, 1(8), 2817-2827. doi:10.1039/C9NA00345B
- OH, T., KIM, M., CHOI, J., & KIM, J. (2018). Design of graphitic carbon nitride nanowires with captured mesoporous carbon spheres for EDLC electrode materials. *Ionics*, 24(12), 3957-3965. doi:10.1007/s11581-018-2544-0
- QIU, H., MA, Q., SUN, X., HAN, X., JIA, G., ZHANG, Y., & HE, W. (2022). Facile synthesis of g-C<sub>3</sub>N<sub>4</sub>/LDH self-growing nanosheet arrays for enhanced supercapacitor performance. *Journal of Alloys and Compounds*, 896, 163023. doi:https://doi.org/10.1016/j.jallcom.2021.163023
- RADHAMANI, A. V., SHAREEF, K. M., & RAO, M. S. R. (2016). ZnO@MnO<sub>2</sub> Core-Shell Nanofiber Cathodes for High Performance Asymmetric Supercapacitors. *ACS Applied Materials & Interfaces*, 8(44), 30531-30542. doi:10.1021/acsami.6b08082
- RADOŃ, A., & ŁUKOWIEC, D. (2018). Silver nanoparticles synthesized by UV-irradiation method using chloramine T as modifier: structure, formation mechanism and catalytic activity. *CrysoEngComm*, 20(44), 7130-7136. doi:10.1039/C8CE01379A
- SHALINI REGHUNATH, B., RAJASEKARAN, S., DEVI K R, S., SARAVANAKUMAR, B., WILLIAM, J. J., PINHEIRO, D., ... KHEAWHOM, S. (2022). Fabrication of bismuth ferrite/graphitic carbon nitride/N-doped graphene quantum dots composite for high performance supercapacitors. *Journal of Physics and Chemistry of Solids*, 171, 110985. doi:https://doi.org/10.1016/j.jpcs.2022.110985
- SHEN, C., LI, R., YAN, L., SHI, Y., GUO, H., ZHANG, J., ... NIU, L. (2018). Rational design of activated carbon nitride materials for symmetric supercapacitor applications. *Applied Surface Science*, 455, 841-848. doi:https://doi.org/10.1016/j.apsusc.2018.06.065
- SIWAL, S., DEVI, N., PERLA, V., BARIK, R., GHOSH, S., & MALLICK, K. (2018). The influencing role of oxophilicity and surface area of the catalyst for electrochemical methanol oxidation reaction: a case study. *Materials Research Innovations*, 1-8. doi:10.1080/14328917.2018.1533268
- SIWAL, S., DEVI, N., PERLA, V. K., GHOSH, S. K., & MALLICK, K. (2019). Promotional role of gold in electrochemical methanol oxidation. *Catalysis, Structure & Reactivity*, 5(1), 1-9. doi:10.1080/2055074x.2019.1595872
- SIWAL, S. S., SHEORAN, K., MISHRA, K., KAUR, H., SAINI, A. K., SAINI, V., ... THAKUR, V. K. (2022). Novel synthesis methods and applications of MXene-based nanomaterials (MBNs) for hazardous pollutants degradation: Future perspectives. *Chemosphere*, 293, 133542. doi:https://doi.org/10.1016/j.chemosphere.2022.133542
- SIWAL, S. S., ZHANG, Q., DEVI, N., & THAKUR, K. V. (2020). Carbon-Based Polymer Nanocomposite for High-Performance Energy Storage Applications. *Polymers*, 12(3). doi:10.3390/polym12030505
- SIWAL, S. S., ZHANG, Q., SUN, C., & THAKUR, V. K. (2019). Graphitic Carbon Nitride Doped Copper-Manganese Alloy as High-Performance Electrode Material in Supercapacitor for Energy Storage. *Nanomaterials*, 10(1). doi:10.3390/nano10010002
- THI, Q. H., MAN, P., HUANG, L., CHEN, X., ZHAO, J., & LY, T. H. (2023). Superhydrophilic 2D Carbon Nitrides Prepared by Direct Chemical Vapor Deposition. *Small Science*, 3(4), 2200099. doi:https://doi.org/10.1002/smsc.202200099
- TYAGI, A., CHANDRA JOSHI, M., AGARWAL, K., BALASUBRAMANIAM, B., & GUPTA, R. K. (2019). Three-dimensional nickel vanadium layered double hydroxide nanostructures grown on carbon cloth for high-performance flexible supercapacitor applications. *Nanoscale Advances*, 1(6), 2400-2407. doi:10.1039/C9NA00152B
- TYAGI, A., JOSHI, M. C., SHAH, A., THAKUR, V. K., & GUPTA, R. K. (2019). Hydrothermally Tailored Three-Dimensional Ni-V Layered Double Hydroxide Nanosheets as High-Performance Hybrid Supercapacitor Applications. *ACS Omega*, 4(2), 3257-3267. doi:10.1021/acsomega.8b03618
- TYAGI, A., MYUNG, Y., TRIPATHI, K. M., KIM, T., & GUPTA, R. K. (2020). High-performance hybrid microsupercapacitors based on Co-Mn layered double hydroxide nanosheets. *Electrochimica Acta*, 334, 135590. doi:https://doi.org/10.1016/j.electacta.2019.135590
- TYAGI, A., SINGH, N., SHARMA, Y., & GUPTA, R. K. (2019). Improved supercapacitive performance in electrospun TiO<sub>2</sub> nanofibers through

- Ta-doping for electrochemical capacitor applications. *Catalysis Today*, 325, 33-40. doi:https://doi.org/10.1016/j.cattod.2018.06.026
- WANG, G., ZHANG, L., & ZHANG, J. (2012). A review of electrode materials for electrochemical supercapacitors. *Chemical Society Reviews*, 41(2), 797-828. doi:10.1039/C1CS15060J
- WANG, H., LIU, Y., KONG, L., XU, Z., SHEN, X., & PREMLATHA, S. (2023). Porous graphitic carbon nitride nanosheets with three-dimensional interconnected network as electrode for supercapacitors. *Journal of Energy Storage*, 63, 106935. doi:https://doi.org/10.1016/j.est.2023.106935
- WANG, X., MAEDA, K., THOMAS, A., TAKANABE, K., XIN, G., CARLSSON, J. M., ... ANTONIETTI, M. (2009). A metal-free polymeric photocatalyst for hydrogen production from water under visible light. *Nature Materials*, 8(1), 76-80. doi:10.1038/nmat2317
- XU, J., YANG, L., CAO, S., WANG, J., MA, Y., ZHANG, J., & LU, X. (2021). Sandwiched Cathodes Assembled from CoS<sub>2</sub>-Modified Carbon Clothes for High-Performance Lithium-Sulfur Batteries. *Advanced Science*, 8(16), 2101019. doi:https://doi.org/10.1002/advs.202101019
- XU, Y., ZHOU, Y., GUO, J., ZHANG, S., & LU, Y. (2019). Preparation of SnS<sub>2</sub>/g-C<sub>3</sub>N<sub>4</sub> composite as the electrode material for Supercapacitor. *Journal of Alloys and Compounds*, 806, 343-349. doi:https://doi.org/10.1016/j.jallcom.2019.07.130
- XUE, J., MA, S., ZHOU, Y., ZHANG, Z., & HE, M. (2015). Facile Photochemical Synthesis of Au/Pt/g-C<sub>3</sub>N<sub>4</sub> with Plasmon-Enhanced Photocatalytic Activity for Antibiotic Degradation. *ACS Applied Materials & Interfaces*, 7(18), 9630-9637. doi:10.1021/acsami.5b01212
- YESMIN, S., DEVI, M., DASGUPTA, R., & DHAR, S. S. (2022). CoFe<sub>2</sub>O<sub>4</sub> nanocubes over Cu/graphitic carbon nitride as electrode materials for solid-state asymmetric supercapacitors. *Chemical Engineering Journal*, 446, 136540. doi:https://doi.org/10.1016/j.cej.2022.136540
- ZHU, H.-L., & ZHENG, Y.-Q. (2018). Mesoporous Co<sub>3</sub>O<sub>4</sub> anchored on the graphitic carbon nitride for enhanced performance supercapacitor. *Electrochimica Acta*, 265, 372-378. doi:https://doi.org/10.1016/j.electacta.2018.01.162
- ZHU, J., KONG, L., SHEN, X., ZHU, G., Ji, Z., XU, K., ... LI, B. (2020). Carbon cloth supported graphitic carbon nitride nanosheets as advanced binder-free electrodes for supercapacitors. *Journal of Electroanalytical Chemistry*, 873, 114390. doi:https://doi.org/10.1016/j.jelechem.2020.114390



**Publisher's note:** Eurasia Academic Publishing Group (EAPG) remains neutral with regard to jurisdictional claims in published maps and institutional affiliations.

**Open Access.** This article is licensed under a Creative Commons Attribution-NonCommercial 4.0 International (CC BY-NC 4.0) licence, which permits copy and redistribute the material in any medium or format for any purpose, even commercially. The licensor cannot revoke these freedoms as long as you follow the licence terms. Under the following terms you must give appropriate credit, provide a link to the license, and indicate if changes were made. You may do so in any reasonable manner, but not in any way that suggests the licensor endorsed you or your use. If you remix, transform, or build upon the material, you may not distribute the modified material. To view a copy of this license, visit <https://creativecommons.org/licenses/by-nc/4.0/>.